Atmos. Chem. Phys. Discuss., 15, 1915–1952, 2015
www.atmos-chem-phys-discuss.net/15/1915/2015/
doi:10.5194/acpd-15-1915-2015

Atmospheric Chemistry and Physics Discussions
Open Access

On the ability of a global atmospheric inversion to constrain variations of CO_2 fluxes over Amazonia

L. Molina[1], G. Broquet[1], P. Imbach[2], F. Chevallier[1], B. Poulter[3], D. Bonal[4], B. Burban[7], M. Ramonet[1], L. V. Gatti[5], S. C. Wofsy[6], J. W. Munger[6], E. Dlugokencky[8], and P. Ciais[1]

[1]Laboratoire des Sciences du Climat et de l'Environnement, CEA-CNRS-UVSQ, IPSL, Gif sur Yvette, France
[2]Climate Change Program, Tropical Agricultural Research and Higher Education Center, Turrialba, Cartago 30501, Costa Rica
[3]Department of Ecology, Montana State University, Bozeman, MT 59717, USA
[4]INRA, UMR EEF, 54280 Champenoux, France
[5]CNEN – IPEN – Lab. Quimica Atmosferica, Av. Prof. Lineu Prestes, 2242, Cidade Universitaria, São Paulo, SP, Brazil
[6]Harvard University, School of Engineering and Applied Sciences, Department of Earth and Planetary Sciences, 20 Oxford Street, Cambridge, MA 02138, USA
[7]INRA, UMR Ecofog, Avenue de France, 97387 Kourou CEDEX, French Guiana
[8]NOAA Earth System Research Laboratory, Global Monitoring Division, Boulder, CO 80305-3337, USA

Received: 1 September 2014 – Accepted: 28 October 2014 – Published: 21 January 2015

Correspondence to: L. Molina (luis.molina@lsce.ipsl.fr)

Published by Copernicus Publications on behalf of the European Geosciences Union.

Abstract

The exchanges of carbon, water, and energy between the atmosphere and the Amazon Basin have global implications for current and future climate. Here, the global atmospheric inversion system of the Monitoring of Atmospheric Composition and Climate service (MACC) was used to further study the seasonal and interannual variations of biogenic CO_2 fluxes in Amazonia. The system assimilated surface measurements of atmospheric CO_2 mole fractions made over more than 100 sites over the globe into an atmospheric transport model. This study added four surface stations located in tropical South America, a region poorly covered by CO_2 observations. The estimates of net ecosystem exchange (NEE) optimized by the inversion were compared to independent estimates of NEE upscaled from eddy-covariance flux measurements in Amazonia, and against reports on the seasonal and interannual variations of the land sink in South America from the scientific literature. We focused on the impact of the interannual variation of the strong droughts in 2005 and 2010 (due to severe and longer-than-usual dry seasons), and of the extreme rainfall conditions registered in 2009. The spatial variations of the seasonal and interannual variability of optimized NEE were also investigated. While the inversion supported the assumption of strong spatial heterogeneity of these variations, the results revealed critical limitations that prevent global inversion frameworks from capturing the data-driven seasonal patterns of fluxes across Amazonia. In particular, it highlighted issues due to the configuration of the observation network in South America and the lack of continuity of the measurements. However, some robust patterns from the inversion seemed consistent with the abnormal moisture conditions in 2009.

1 Introduction

The forests of Amazonia cover 6.77 million km^2 (INPE, 2011). It is the world's largest continuous area of tropical forest and reservoir of aboveground organic carbon (Malhi

ACPD
15, 1915–1952, 2015

et al., 2008). Changes in the carbon dynamics of this ecosystem thus have global significance (Wang et al., 2013). However, the natural variability of CO_2 exchange in Amazonia, as well as its short and long term response to natural and anthropogenic disturbance across scales, is still poorly understood and is the topic of active research.

There is intense debate about the timing and magnitude of the seasonal cycle of CO_2 fluxes across Amazonia. Studies employing remote sensing data as a proxy for canopy photosynthetic activity have suggested a widespread enhancement of gross primary productivity (GPP) of the Amazonian rainforest during the dry season (Huete et al., 2006). Yet, direct and continuous measurements of net ecosystem exchange (NEE) between the atmosphere and forest canopy at a local scale (from 1 ha to 1 km^2 scale) based on eddy-covariance (EC) systems do not support such large-scale behaviour. Several EC observations in central eastern Amazonia (Saleska et al., 2003) and north-eastern Amazonia (Bonal et al., 2008) also indicate that tropical forest areas take up CO_2 during the dry season, but similar EC studies in central Amazonia have suggested an opposite seasonality (Grace et al., 1996; Araújo et al., 2002). Finally, remote sensing measurements of the vertically integrated columns of CO_2 (XCO_2) retrieved from the GOSAT satellite, suggest stronger CO_2 uptake during the wet season in southern Amazonian forest than during the dry season (Parazoo et al., 2013). These measurements thus reveal a large heterogeneity in space of the phase of the seasonal cycle of NEE within Amazonia. However, most dynamic global vegetation model (DGVM) simulations predict stronger uptake during the wet season throughout Amazonia (Verbeeck et al., 2011; Saleska et al., 2003; Baker et al., 2008; Poulter et al., 2009); although limitations related to mortality or land use, do restrict the ability of these generic global models to simulate CO_2 fluxes and carbon stocks of Amazonian forest (Gloor et al., 2012).

Uncertainty associated with potential spatial heterogeneity is also apparent in the estimates of the interannual variability (IAV) of CO_2 fluxes in Amazonia, in particular during years with extreme climatic conditions. Remote sensing observations during the severe Amazonian drought of 2005 suggested a widespread enhancement of photo-

ACPD
15, 1915–1952, 2015

synthetic activity, or greening, across Amazonia (Saleska et al., 2007). The resilience of forests to water stress suggested by the "drier-yet-greener" papers was originally attributed to a combination of deep rooting, hydraulic redistribution, and more available solar radiation (Saleska et al., 2007). However, the validity of enhanced vegetation index (EVI) satellite data has been recently challenged by Morton et al. (2014) and by losses in canopy functioning detected in radar-based measurements (Saatchi et al., 2012). The observations from optical satellite sensors remain controversial because other studies did not find such an impact on Amazonian forest (Xu et al., 2011; Samanta et al., 2010, 2012). Moreover, observations of microwave backscatter from QuickSCAT have suggested large-scale, persistent negative effects of the drought of 2005 on forest canopy structure (Saatchi et al., 2012). Biometry measurements, consisting of periodic measurements of the allocation of photosynthetic products to wood growth, provide another perspective on the effects of drought on Amazonian forest trees. In a large-scale, long-term biometric study, Phillips et al. (2009) found a reversion of the carbon sink due to the effect of the drought of 2005 on tree mortality. This is consistent with a synthesis of yearly estimates of natural fluxes (NEE plus biomass-burning emissions) from an ensemble of DGVMs compiled at http://www.globalcarbonatlas.org).

The scientific community has used atmospheric inversions for more than two decades in an effort to improve the knowledge of CO_2 fluxes at large scale. Whereas EC or biometric studies give flux estimates that are valid at local scale (Ometto et al., 2005), atmospheric inversion offers the possibility to derive measurement-based estimates for the whole of Amazonia, with spatial resolutions larger than 500 km, provided that atmospheric observations can adequately sample the Amazonian flux signal. Inversions use available measurements of atmospheric CO_2 to provide corrections to prior surface flux estimates using an atmospheric transport model and statistical inversion methods. The method estimates statistically optimal fluxes within the boundaries of uncertainties in the measurements and prior flux estimates (Enting et al., 1995; Ciais et al., 2010). The flux corrections are applied by the inversion system to prior fluxes to which measurements are sensitive in space and time (as a function of the atmospheric

ACPD
15, 1915–1952, 2015

transport), and are extrapolated beyond the vicinity of the measurement footprint by the system through hypotheses on the spatial and temporal correlation of the uncertainties in the prior fluxes. Peylin et al. (2013) show that the different inverted seasonal cycles and IAVs of natural CO_2 fluxes from several state-of-the-art global atmospheric inversions are characterized by a large scatter over tropical South America (TSA). This is explained by the variety of prior estimates used by the different global inversion systems, and by the large-scale corrections that are applied in regions poorly covered by observation networks, such as TSA, in order to balance the global CO_2 budget, rather than to match local measurements. For these reasons, atmospheric inversions have not been included in the review of the carbon cycle in South America made by Gloor et al. (2012). Lloyd et al. (2007) and Gatti et al. (2010) applied the principle of atmospheric inversion to exploit vertical CO_2 profile data from airborne measurements in Amazonia. Their studies, based on measurements near Manaus, in central Amazonia (Lloyd et al., 2007), and Santarém in eastern Amazonia (Gatti et al., 2010), constitute important efforts to constrain surface CO_2 fluxes at regional scale, measuring and exploiting some of the few atmospheric data sets available for South America. Their results suggested CO_2 efflux from the ecosystem during the wet season in eastern Amazonia. The recent study of Gatti et al. (2014), using vertical profiling of air columns, collected approximately every two weeks, over the two-year period 2010–2011, provides a basin-scale picture that confirms this regional signal, but suggests the inverted pattern in southern and western Amazonia. Their study reported on the first estimate of CO_2 fluxes for the whole Amazon basin, in an unprecedented effort that overcame limitations of both local and model-based estimates of CO_2 fluxes in Amazonia (Balch, 2014); it provides an insight into the sensitivity of this important ecosystem to moisture stress, and suggests the importance of including such estimates over longer time periods.

Our goal here is to study the seasonal cycle and IAV of NEE over Amazonia during 2002–2010. This period offers the opportunity to investigate significant anomalies in the interannual variability of carbon fluxes, particularly those associated with the severe droughts of 2005 and 2010, and with the extreme rainfall registered across the

ACPD
15, 1915–1952, 2015

Amazon basin in 2009 (Marengo et al., 2010). The study is based on the MACC inversion system initially described by Chevallier et al. (2010) (hereafter CH2010). We used v10.1 of the MACC CO_2 inversion product released in August 2011. We added four ground-based atmospheric measurement sites surrounding the northeast of Amazonia to the assimilated data. Despite the limitations of this approach in South America, highlighted above and by Gloor et al. (2012), this new attempt at characterizing temporal variations in the NEE over Amazonia based on atmospheric inversions, can be justified by the use of these stations located in the region. In particular, we are the first to use continuous measurements from French Guyana: the impact of this inclusion can be assessed through comparisons with inversions ignoring these sites. The use of these stations was expected to increase significantly the sampling of the atmospheric signature of the fluxes in Amazonia. Moreover, when global inversions do not assimilate data from this region, they produce large increments of NEE in Amazonia – the reliability of these modelled fluxes should be analyzed.

Our analysis of the inversion results was compared to the independently derived NEE estimated by Jung et al. (2011) (hereafter J2011). J2011 used model tree ensembles, a machine-learning technique, to upscale FLUXNET eddy-covariance observations, based on remote sensing, climate, and land-use data as drivers, thereby producing gridded estimates of NEE and other surface fluxes at the global scale at 0.5° resolution. As discussed in J2011, large uncertainties affect their annual mean NEE estimates and associated seasonal and interannual variations. This is likely particularly true in TSA, were few FLUXNET measurements are available. Yet, its comparison to the NEE from the inversion could give useful insights for the analysis of the latter.

The rest of this paper is structured as follows. We present each component of the inversion setup in Sect. 2, the results of the inversion and their comparison to the standard MACCv10.1 inversion (not constrained by the four stations positioned around Amazonia) as well as to J2011 in Sect. 3. In Sect. 4, we discuss the results and conclude the study.

2 The inversion method

This study builds on the global atmospheric inversion framework of CH2010 to correct a prior estimate of NEE from the model ORCHIDEE (Organizing Carbon and Hydrology in Dynamic Ecosystems, Krinner et al., 2005) and of ocean fluxes, based on the assimilation of in situ measurements of atmospheric CO_2 mole fractions into a global atmospheric transport model. The approach relies on a Bayesian framework to estimate the conditional probability of the "true" NEE and ocean fluxes given the statistical information from the prior fluxes and the set of in situ measurements of atmospheric CO_2 (henceforward observations). Assumption of unbiased Gaussian distribution of the uncertainties in the prior fluxes and those underlying the simulation of the observations using the transport model, allows us to derive an updated estimate of NEE and ocean fluxes (hereafter the posterior fluxes) that also has an unbiased Gaussian distribution. The statistically optimal fluxes (i.e., the mean of the posterior distribution of the fluxes) are found by calculating the minimum of the cost function (Tarantola, 2005)

$$J(\boldsymbol{x}) = (\boldsymbol{x} - \boldsymbol{x}^{\mathrm{b}})^{\mathrm{T}}\mathbf{B}^{-1}(\boldsymbol{x} - \boldsymbol{x}^{\mathrm{b}}) + (\boldsymbol{y}^{\mathrm{o}} - H\boldsymbol{x})^{\mathrm{T}}\mathbf{R}^{-1}(\boldsymbol{y}^{\mathrm{o}} - H\boldsymbol{x}) \quad (1)$$

where $\boldsymbol{x}$ is the control vector and mainly denotes the NEE (defined as the difference between the gross CO_2 uptake through photosynthesis and output through total ecosystem respiration), and air–ocean exchanges that are optimized at a chosen spatial and temporal resolution. $\boldsymbol{x}^{\mathrm{b}}$ represents the prior NEE and ocean fluxes, and $\boldsymbol{y}^{\mathrm{o}}$ is the vector of observations. H is the operator projecting $\boldsymbol{x}$ into the observation space, and is based on an atmospheric transport model and fossil fuel and biomass-burning CO_2 emission estimates. $\mathbf{B}$ and $\mathbf{R}$ are the covariance matrices of the normal distribution of the uncertainty on $\boldsymbol{x}^{\mathrm{b}}$ and of the sum in the observation space of the other uncertainties when comparing $H\boldsymbol{x}^{\mathrm{b}}$ to $\boldsymbol{y}^{\mathrm{o}}$, respectively. The latter includes the measurement, model transport and model representation errors. A complete solution to the inversion problem requires the estimation of the uncertainty in the optimized fluxes. This estimation was not performed in this study since it would have been highly demanding in terms of

ACPD
15, 1915–1952, 2015

computation. CH2010 provides details on this estimation and typical results of uncertainty reduction that should be nearly valid here for regions outside TSA. The following sections present a brief description of each component of the inversion configuration used in this study, while CH2010 provides more details.

2.1 Inversion modelling setup

Following CH2010, the link between CO_2 fluxes and observations was simulated by the global circulation model of the Laboratoire de Météorologie Dynamique (LMDZ) (version 4, Hourdin et al., 2006), which is the atmospheric component of the coupled climate model of the Institut Pierre Simon Laplace IPSL-CM4. Tracer transport was simulated by LMDZ at a horizontal resolution of $3.75^\circ \times 2.75^\circ$ (longitude × latitude) and with a vertical resolution of 19 levels between the surface and the top of the atmosphere. LMDZ was nudged to winds modelled by the European Centre for Medium-Range Weather Forecasts (ECMWF).

Prior NEE in MACCv10.1 was estimated at $3.75^\circ \times 2.75^\circ$ and 3 h resolution from a global simulation of the ORCHIDEE model at 0.7° resolution by Maignan et al. (2011). ORCHIDEE was forced with the atmospheric conditions of ECMWF reanalysis ERA-Interim (Berrisford et al., 2009). Here ORCHIDEE NEE does not take into account disturbance from land use or wildfires. Prior ocean–atmosphere CO_2 exchanges were obtained from the climatology of air–ocean CO_2 partial pressure difference by Takahashi et al. (2009).

To complement these fluxes that were controlled by the inversion, the *H* operator also included fixed estimates of the fossil fuel and biomass-burning CO_2 emissions. Fossil fuel emissions were obtained from the EDGAR-3.2 Fast Track 2000 database (Olivier and Berdowski, 2001), scaled annually with the global totals of the Carbon Dioxide Information Analysis Center (CDIAC). CO_2 emissions from biomass burning were taken from the Global Fires Emission Database version 2 (GFEDv2, Randerson et al., 2007). Assuming that the vegetation recovers rapidly from fire events, the CO_2

ACPD
15, 1915–1952, 2015

emissions from fires that affected the vegetation in a given year were offset by an equivalent, compensatory regrowth CO_2 uptake evenly distributed throughout the year.

The inversion controlled 8-day mean daytime and nighttime NEE and 8-day mean ocean fluxes at the spatial resolution of the transport model. The analysis in this study focused on NEE, thus the impact of the inversion on ocean fluxes was not examined. At the grid scale, uncertainties in the prior NEE are estimated as proportional to the heterotrophic respiration fluxes from ORCHIDEE. Spatial correlations of the uncertainties in **B** decay exponentially as a function of the distance between corresponding pixel-based estimates of the fluxes with a length scale of 500 km for NEE (1000 km for ocean fluxes). Temporal correlations of the uncertainties decay exponentially as a function of the lag-time between the corresponding 8-day mean daytime or nighttime estimate of the fluxes with a timescale of one month, but without correlation between daytime and nighttime uncertainties. The resulting correlations in **B** are estimated as the product between the temporal and the spatial correlations. This setup of the correlations for **B** is based on the estimates by Chevallier et al. (2006) of differences between the NEE simulated by ORCHIDEE and EC flux measurements. However, their study used EC data from flux towers mostly located in the Northern Hemisphere, and thus the resulting estimation of correlation might not apply well to ecosystems in tropical Amazonia.

In the inversion framework, the misfits between simulated CO_2 mole fractions and the measurements that are not due to uncertainty in the prior NEE or ocean fluxes must be accounted for in the covariance matrix **R**. Uncertainties in fire and anthropogenic CO_2 emissions are assumed to have negligible impact at the measurement locations used here. Therefore, they are ignored in the setup of **R**. Following CH2010, the measurement errors are assumed to be negligible in comparison to the uncertainties in the transport model. Model transport and representation errors are modelled as half the variance of the high frequency variability of the deseasonalized and detrended CO_2 time series of the measurement at a given station.

ACPD
15, 1915–1952, 2015

On the ability of a global atmospheric inversion to constrain variations of CO_2 fluxes over Amazonia

L. Molina et al.

2.2 Assimilated data

MACCv10.1 assimilated measurements of atmospheric CO_2, expressed as dry air mole fractions in $\mu mol\,mol^{-1}$ (abbreviated ppm), from 128 surface sites: 35 continuous measurement stations and measurements of CO_2 from discrete air samples collected approximately weekly at 93 sites. Out of all the stations, 29 were located in the tropics (but only two of these stations had continuous measurements) but none of these tropical stations were located in TSA. In this study we added new data from four surface sites located in this region. Figure 1 maps the measurement stations used by MACCv10.1 and the four stations added in this study. At Arembepe (ABP), data consist of weekly measurements of atmospheric CO_2 with discrete air samples. At the other three stations, CO_2 was measured with continuous analyzers and data were reported as hourly averages of these measurements at Santarém (SAN) and Guyaflux (GUY), and 30 min averages at Maxaranguape (MAX). Figure 2 illustrates the temporal coverage of the observations available in TSA during the simulated period (2002–2010). There is little overlap among the site records, due to calibration problems, interruption of the measurements (e.g., at MAX) and the fact that some stations have been setup only recently (e.g., at GUY). The longest records were from ABP, with data spanning November 2006 to December 2010, and SAN, covering January 2002 to December 2005. At MAX the information covered the periods July 2004 to May 2005 and mid-September 2006 to December 2006. GUY is the most recent station, with data covering October 2009 to December 2010.

Figure 3 depicts average wind fields in February over 2002–2010, which illustrates the typical circulation pattern. Winds convey air masses entering from the Atlantic Ocean near the Equator across the continent and back into the southern Atlantic Ocean generally south of 20° S. This pattern of advective transport suggests that the variations of CO_2 at coastal stations (ABP, MAX) are influenced by air–ocean exchanges and fluxes in distant lands. These stations thus provide more information on the relatively homogeneous background atmospheric CO_2 content upwind of TSA, than on the

ACPD
15, 1915–1952, 2015

fluxes within Amazonia. On the other hand, stations like GUY and SAN receive a signal from ecosystems in the northeastern Amazon Basin. Despite GUY being not far from the coast considering the Amazon-wide scale, this site is actually located in an area covered by undisturbed, tropical wet forest (Bonal et al., 2008). SAN is located considerably further inland than GUY. Typical influence functions of fluxes for observations at GUY and SAN (Fig. 3b and c, respectively) illustrate that the sensitivity of instantaneous mole fractions to fluxes decreases rapidly with distance mainly due to the typically moderate horizontal wind speeds, so that they should bear a strong signature of local fluxes i.e., of the NEE in northeastern Amazonia. To further evaluate the sensitivity of these four stations to the pattern of interest in the regional NEE, we estimated the difference between CO_2 mole fractions modelled using the standard prior NEE of the system and an NEE estimate called "flat prior". The flat prior was built by applying an annual offset to the prior NEE of MACCv10.1 so that the interannual variations of annual budgets become null. This annual offset was calculated as the difference between the mean flux for a given year over the whole region and the mean flux over the simulation period and the entire study area. Thus, the flat prior interannual anomalies were null but the spatial the temporal variability at scales smaller than a year were preserved. The root mean square of the annual biases ranges from 0.39 ppm (GUY and MAX) to 0.60 ppm (SAN). This shows that the signature of the interannual variability of the NEE in Amazonia should be easy to filter out from the measurement time series given that the mean transport error at the yearly scale should be far smaller according to the hypothesis made when setting-up the inversion system. Therefore, this supported the attempt at controlling the interannual variability of the NEE in Amazonia through the inversion using the observations from the four sites in TSA.

We assimilated observations between 12:00 and 15:00 local time (LT), when the boundary layer (BL) is well developed and likely to be better represented by the transport model (Butler et al., 2010; Gatti et al., 2010). This should avoid the difficulties the transport model has in simulating nighttime stratification, and morning and evening transitions in the BL diurnal cycle. Observations were also screened for low wind speed

ACPD
15, 1915–1952, 2015

($> 2\,\mathrm{m\,s^{-1}}$), thus removing the effect of local emissions (and sinks) that may not be well captured by the transport model at $3.75^{\circ} \times 2.5^{\circ}$ resolution and to monitor the signal of fluxes at larger scales.

3 Results

In this section we first analyze the statistical misfits between observations and simulated mole fractions from prior and posterior fluxes, as a measure of the efficiency of the inversion in reducing the misfits to the measurements. This is a first indicator of the significance of the corrections applied to the fluxes. We then examine the impact of inversion on the seasonal patterns and IAV of NEE. This analysis was supported by the comparison to the product of J2011.

3.1 Comparison to observed CO_2 mole fractions

The time series of assimilated observations and the corresponding simulated CO_2 mole fractions using the prior fluxes, the inverted fluxes from MACCv10.1 and our inverted fluxes (henceforth INVSAm) are plotted in Fig. 4. The statistics for bias and mean error between measured and simulated CO_2 mole fractions for the four stations in South America are summarized in Fig. 5. Although the information from these four stations seems to critically reduce a large-scale bias over TSA, the presence of a few marine stations on the globe is enough to introduce this effect by correcting the global growth rate of CO_2 (CH2010). However, the information from the local network significantly impacted the seasonality of simulated CO_2. The resulting optimized mole fractions from INVSAm generally shifted from minima to maxima around June every year at SAN or from maxima to minima around October and April at MAX with respect to the prior fluxes and MACCv10.1 (Fig. 4c) and in agreement with the observations. While yielding a phase of seasonality at GUY comparable to that of the prior fluxes and MACCv10.1, INVSAm exhibited a significant rescaling of the seasonal variations in the period from

ACPD
15, 1915–1952, 2015

May to September at GUY (Fig. 4b) compared to these two other simulations; this was in agreement with the observations. At ABP, INVSAm surprisingly yielded an amplitude of the decrease of concentrations between January and May in 2007 and 2009 at ABP that was higher than that of the observations and of MACCv10.1, even though smaller than that of the prior flux simulations (Fig. 4a).

Subsequently, when compared to MACCv10.1, INVSAm improved the amplitude of the variations of the simulated mole fractions with respect to the prior flux simulation at GUY and MAX and did not impact it at SAN, but degraded it at ABP, even though, as well as MACCv10.1, it still provided a better amplitude of the variations than that of the prior flux simulations at all sites. The best correlations with the observations were obtained with INVSAm except at ABP, but the values remained low in all cases, ranging from 0.23 at GUY to 0.79 at MAX.

These results suggest that the inversion of data in South America helped improve the phasing of the seasonal variations compared to the data, whereas MACCv10.1 did not impact it, except at ABP. MACCv10.1 mainly decreased the biases and improved the amplitude of the seasonal variations only. There is thus some hope of having improved the seasonal variations of the NEE in INVSAm. However, the rather low values of correlations to the data and the large remaining discrepancies in the data, even when using INVSAm, may reveal that this improvement is not significant enough. Furthermore, results at ABP may reveal some local issues. Finally, given the very large bias from the prior flux simulation being mainly related to an erroneous global growth rate, and the inversion having varying efficiency to decrease it depending on the sites or on the year, it seems hard to interpret part of this decrease as a result of improvement of the interannual variability in the NEE.

ACPD
15, 1915–1952, 2015

3.2 Diagnostics of the biogenic CO_2 fluxes

3.2.1 Seasonality

Figure 6a illustrates the mean seasonal cycle of NEE from the prior fluxes, J2011, MACCv10.1 and INVSAm over TSA. The mean for the full period 2002–2010 was removed because uncertainties in the long-term mean can be large for the inversions as well as for the J2011 product, and because this long-term mean can differ significantly between the different estimates. Removing the means allows us to focus on the seasonal variations. Hereafter, positive values of NEE indicate anomalous CO_2 release to the atmosphere; negative values indicate anomalous uptake by the ecosystems. The shaded area indicates the dry season, defined as months with precipitation < 100 mm according to data from the Tropical Rainfall Measuring Mission (TRMM 3B43 (v6) product), averaged over January 2002 to June 2010. The results of Fig. 6a were calculated considering all the plant functional types (PFTs) represented in ORCHIDEE over the study region. The vegetation map of ORCHIDEE, originally at a spatial resolution of 0.72°, was aggregated according to the transport model grid, and Fig. 7 illustrates the dominant PFTs in terms of area for each transport model grid cell.

Both the prior flux simulation and the inversions predicted a maximum of NEE (i.e., likely a maximum of CO_2 release) in the dry season and a minimum of NEE (i.e., likely a maximum of CO_2 uptake) in the wet season (Fig. 6a). This behaviour was also observed in J2011. However, J2011 indicated the maximum of NEE during the transition between the wet and dry season while the prior flux simulation and the inversions indicated that it occurs at the end of the dry season. Even though the inversions seemed to delay or lengthen this maximum, such a modification was not significant and their seasonal phasing was likely strongly constrained by the patterns of the prior fluxes. In particular, according to the comparison between INVSAm and MACCv10.1, the assimilation of data from the four stations in South America did not seem to impact this phasing. However, such data are prone to bring a constraint on fluxes mainly in tropi-

Discussion Paper | Discussion Paper | Discussion Paper | Discussion Paper |

ACPD

15, 1915–1952, 2015

On the ability of a global atmospheric inversion to constrain variations of CO_2 fluxes over Amazonia

L. Molina et al.

cal broadleaf evergreen and raingreen (TBE) forests (Fig. 7), while the mean seasonal behaviour over the whole analyzed domain could be mainly related to other PFTs.

Therefore, we isolated the results for TBE forests and calculated the mean seasonal cycle of NEE over model grid cells dominated by this vegetation type (Fig. 6b). This did not yield any clear correlation between the existence of maxima or minima in NEE and the phasing of wet and dry seasons, neither when considering the NEE from the prior nor when considering the NEE from both inversions estimates, even though J2011 indicates a maximum of the NEE a few months before the beginning of the dry season and a minimum of the NEE at the beginning of the wet season. In particular, the prior and the inversions indicated several local maxima or minima in the NEE. This could reflect the signature of the overlapping of significantly different seasonal cycles for different sub-regions.

The strong spatial heterogeneity of the time variations of the NEE in TBE forests, which has been discussed in the introduction, is illustrated here along with the spatial heterogeneity of the time variations of the precipitation in Fig. 6c–f. Figure 6c–f are based on monthly averages of NEE measurements at four flux towers located in central eastern, and southern Amazonia (Fig. 7). The sites at Caxihuanã (BR-Cax, Fig. 6c) and Rebio Jarú (BR-Ji2, Fig. 6f) are covered by *terra firme* humid forest; the sites are described by Carswell et al. (2002) and von Randow et al. (2004), respectively. Data cover the period 2000–2002 at both sites. At Santarém (BR-Sa3, Fig. 6e), data shown were collected at the Tapajós km 83 tower site, an area covered by tropical humid forest, over 2001–2002. A description of the site can be found in Goulden et al. (2004) and Miller et al. (2004). The site at Bananal Island (BR-Ban, Fig. 6a), on the other hand, is located in a floodplain, in an area of transition between forest and savannah vegetation (Borma et al., 2009). At BR-Ban data cover the period 2004–2005. At these four sites, mean NEE was removed. To examine if the inversion captured this spatial variability of the fluxes, we analyzed the seasonal variations of the NEE estimates for the two zones depicted in Fig. 7. Zone 1 was located in northeastern Amazonia, close to the measurement stations SAN and GUY. Zone 2 was located in central eastern

ACPD
15, 1915–1952, 2015

Amazonia. Both zones were mainly covered by TBE forests, according to the vegetation classification of ORCHIDEE. According to Malhi et al. (2009), eastern Amazonia is drier, and shows a stronger seasonality than western Amazonia. However, we did not identify a clear pattern of NEE seasonal variations that could be driven by the rainfall seasonality in any of the two sub-regions, except for J2011 in Zone 1 (Fig. 6g), since the other model estimates exhibited, again, maxima and minima of NEE during both dry and wet seasons. Actually, in Zone 2 (Fig. 6h) the dry season could not be clearly identified. In this zone, the prior flux and the inversions indicated several maxima and minima of NEE, but J2011 exhibited, again, a clear seasonal cycle with a maximum in June and a minimum October as in Zone 1. While J2011 showed nearly the same amplitude and phasing of monthly mean NEE variations in both zones and over TBE forests (Fig. 6b), prior and inversions estimates of the seasonal variations differed both in phasing and amplitude between zone 1, 2 and the whole TBE forest area.

Divergent patterns could be found in INVSAm with respect to MACCv10.1, which remained closer to the prior fluxes. The comparison of these inversion results showed that significant flux corrections due to the assimilation of data in South America were applied in Zone 1 (Fig. 6h), i.e., in northeastern Amazonia, where the stations SAN and GUY were located.

In an attempt at getting clearer seasonal patterns in some of the sub-regions of Amazonia, two additional zones were analyzed, located in southwestern and southeastern Amazonia. Both sub-regions encompassed areas where the impact of the droughts of 2005 and 2010 was the highest according to Lewis et al. (2011). The results, however, are not shown here since the results did not provide further information than is given in zones 1 and 2. J2011 still exhibited the same amplitude of the seasonal cycle and the same location of maximum and minimum NEE as in zones 1 and 2 despite the extent of the dry season. Prior fluxes and inversions still showed maxima and minima during the dry season in some cases, and inversions introduced only slight modifications to the amplitude and phasing of the NEE relative to the prior simulation.

ACPD
15, 1915–1952, 2015

Figure 8 shows the spatial distribution of the corrections applied by INVSAm and depicts large zones of contiguous negative and positive flux increments. When the mean corrections were positive (respectively negative), e.g., during July (respectively during February) in the area of the measurements sites (in the north of South America, which overlap the Zone 1 defined in Fig. 7), negative (respectively positive) corrections were applied south of this area (including the Zone 2 defined in Fig. 7), which seems to underlie the need for the inversion to balance the overall corrections in tropical South America in order to fit the measurements outside the continent. Such dipoles are a typical behaviour of inverse modelling systems in data-poor regions (Peylin et al., 2002). This may be related to the setup of the uncertainties in the prior covariance matrix that would not perfectly fit with actual errors in the prior estimate, and that may extend the corrections too far from the measurement footprints. This questions the spatial variations of the corrections applied by the inversion to the seasonal cycle of the NEE.

3.2.2 Interannual variability

Figure 9a depicts annual NEE anomalies of the prior simulation, MACCv10.1, INVSAm and an additional inversion called FLAT, compared to the mean of 2002–2010, aggregated over the whole study region (considering all PFTs). FLAT corresponds to the inversion using the flat prior described in Sect. 2.2, and whose annual anomalies are null over the whole study region. Prior fluxes, MACCv10.1 and INVSAm predicted only small positive anomalies during the years of drought (2005, 2010) compared to other years. FLAT predicted a negative anomaly (i.e., a strong uptake) in 2010, but it indicates a larger positive anomaly in 2005 than that of other estimates.

On the other hand, the strong NEE negative anomaly of 2009 in the prior fluxes, MACCv10.1 and INVSAm was also predicted by FLAT, which suggests a robust pattern strongly driven by the atmospheric measurements.

As in Sect. 3.2.1, we isolated the results for the TBE forests (Fig. 9b). In this case, prior fluxes and both MACCv10.1 and INVSAm estimates predicted diverging annual mean responses of forests to drought, with a positive anomaly in 2005 and a negative

Discussion Paper | Discussion Paper | Discussion Paper | Discussion Paper |

ACPD

15, 1915–1952, 2015

On the ability of a global atmospheric inversion to constrain variations of CO_2 fluxes over Amazonia

L. Molina et al.

anomaly in 2010. In 2009, when climatic conditions were abnormally humid across South America, the inversion estimates consistently predicted a small positive anomaly. The small anomalies in all inversions suggest a weak sensitivity of the NEE of TBE forests to interannual variations and that most of the IAV over the study area is not related to TBE forests.

Finally, we analyzed the results in the two sub-regions shown in Fig. 7, in an attempt to identify potential differences in the regional responses. NEE estimates from the prior, INVSAm and MACCv10.1 showed various responses of forests to drought in these zones. In zone 1 (Fig. 10a) all these estimates showed a positive anomaly in 2005 and a negative anomaly in 2010, while in zone 2 (Fig. 10b) they yielded negative anomalies during both years. J2011 exhibited abnormal anomalies much smaller than these NEE estimates (Fig. 10c and d), which prevents us from getting insights on the IAV from the comparison of J2011 to the other estimates.

4 Discussion and concluding remarks

Amazonian forest plays a key role in the global carbon balance, but there are large uncertainties on the evolution of this terrestrial sink. Uncertainties stem from the incomplete knowledge of the processes behind land–atmosphere CO_2 exchange in this type of forest. Improving our understanding of the seasonal and interannual variations of Amazonian forest is thus a priority. In an attempt to gain insight into how these temporal variations of CO_2 fluxes vary across Amazonia, we incorporated new measurements of atmospheric CO_2 mole fractions in TSA into a global atmospheric inversion.

Despite an overall improvement by the inversion of the seasonal variations of the simulated concentrations when compared to the measurements in TSA, several issues arose when analyzing the seasonal cycles of NEE from the inversion. The prior and inversion estimates of this mean seasonal cycle of NEE at basin scale were not in line with J2011 and disagreed with the intuitive assumption that the seasonal cycle should be correlated with rainfall and solar radiation, especially in the tropical forest

ACPD
15, 1915–1952, 2015

area. Furthermore, they did not exhibit a clear seasonal pattern over TBE forests at basin scale or within the analyzed sub-regions. J2011 yielded a clear, homogeneous seasonal cycle all over the domain, which does not give confidence in its ability to distinguish regional heterogeneity.

The proximity of Zone 1 to the stations in northeastern Amazonia (SAN and GUY) (Fig. 7) suggested a better confidence in the flux corrections applied by INVSAm to the prior fluxes in that zone than elsewhere in the study area, especially since the analysis of the spatial distribution of such corrections over the whole study area in Fig. 8 gave low confidence in the corrections applied south of the measurement site area, and which seems to artificially balance the overall correction in tropical South America.

The dipoles likely identified in Fig. 8 are characteristic of domains that are poorly constrained by atmospheric data in inversion studies (Peylin et al., 2002). The footprint in the flux space of the set of four stations in South America used in this study covered a very limited area of Amazonia. This suggests that the extrapolation of the information from this area to the whole of Amazonia relies on statistics of the uncertainty in the prior fluxes, for which the reliability is relatively low, and on the need to balance the overall correction over TSA to fit the measurements made outside this region. Furthermore, with limited overlap among the TSA observations, the inversion system may have applied corrections in response to events registered by only a single station at a time. The reliability in the seasonal patterns of the inverted fluxes is thus not high.

Such considerations also weaken the analysis of the IAV based on the inversion while J2011 does not provide a reliable IAV of the NEE in TSA, which could have supported such an analysis. But some patterns of the IAV in the NEE from the inversion seem robust and strongly driven by the atmospheric measurements: across Amazonia the estimates from the prior fluxes, MACCv10.1, INVSAm and FLAT indicate small positive flux annual anomalies (CO_2 release) during the drought in 2005 and a strong negative (CO_2 sink) anomaly in 2009, presumably related to lower temperatures and more humid conditions in 2009. However, in 2010 there is a divergence of the results between the FLAT estimate and the others.

ACPD
15, 1915–1952, 2015

In the TBE forest, the highest source anomaly in 2005 seen in the prior fluxes, MACCv10.1 and INVSAm may be related to reduced photosynthesis during the drought, as found by Gatti et al. (2014), and/or tree mortality caused by a squall event of January 2005 Negrón-Juárez et al. (2010). However, in 2010 these results indicate a small sink anomaly. This anomaly seems inconsistent with the hypothesis of a higher negative impact of the drought in 2010, which was more intense in terms of water stress and more geographically extensive (Lewis et al., 2011). On the other hand, it seems consistent with the recent results of Gatti et al. (2014), who found that the Amazon basin was carbon neutral during that year.

Even though some seasonal or interannual patterns from the inversion could look realistic, our study mainly reveals some critical issues that hamper the ability to derive an accurate estimation of the temporal variability of NEE and of its spatial heterogeneity across Amazonian forests. A denser monitoring network across the basin, with continuous time series, as done by Gatti et al. (2014), is essential to better constrain the fluxes in the region. In addition, the simulation of atmospheric transport in this region needs to be handled using models that are better adapted to the local meteorological conditions. Regional transport models with higher spatial and temporal resolution and improved parameterizations of key atmospheric processes for the region (e.g., deep convection, Parazoo et al., 2008) have been developed (Moreira et al., 2013). The combination of a denser observation network and state-of-the-art regional modelling tools would overcome some of the critical limitations encountered here for the study of the temporal variability of biosphere CO_2 fluxes in Amazonia.

Acknowledgements. We would like to thank Martin Jung (Max Planck Institute for Biogeochemistry) for the access to the upscaled NEE data. This study was part of the GUYAFLUX project funded by the French Ministry of Research, INRA, and the CNES, in the framework of the PO Feder Région Guyane. This study was co-funded by the European Commission under the EU Seventh Research Framework Programme (grant agreement No. 283080, Geocarbon project) and ARIA Technologies. G. Broquet acknowledges funding and support from the Chaire industrielle BridGES, a joint research program between Thales Alenia Space, Veolia, CEA, UVSQ and CNRS.

ACPD
15, 1915–1952, 2015

References

Araújo, A. C., Nobre, A. D., Kruijt, B., Elbers, J. A., Dallarosa, R., Stefani, P., von Randow, C., Manzi, A. O., Culf, A. D., Gash, J. H. C., Valentini, R., and Kabat, P.: Comparative measurements of carbon dioxide fluxes from two nearby towers in a central Amazonian rainforest: the Manaus LBA site, J. Geophys. Res., 107, 8090, doi:10.1029/2001JD000676, 2002. 1918

Baker, I. T., Prihodko, L., Denning, A. S., Goulden, M., Miller, S., and da Rocha, H. R.: Seasonal drought stress in the Amazon: reconciling models and observations, J. Geophys. Res., 113, G00B01, doi:10.1029/2007JG000644, 2008. 1918

Balch, J. K.: Atmospheric science: drought and fire change sink to source, Nature, 506, 41–42, doi:10.1038/506041a, 2014. 1920

Berrisford, P., Dee, D., Fielding, K., Fuentes, M., Kallberg, P., Kobayashi, S., and Uppala, S.: The ERA-Interim archive, Tech. rep., European Centre for Medium Range Weather Forecasts, Reading, 2009. 1923

Bonal, D., Bosc, A., Ponton, S., Goret, J.-Y., Burban, B., Gross, P., Bonnefond, J.-M., Elbers, J., Longdoz, B., Epron, D., Guehl, J.-M., and Granier, A.: Impact of severe dry season on net ecosystem exchange in the neotropical rainforest of French Guiana, Glob. Change Biol., 14, 1917–1933, doi:10.1111/j.1365-2486.2008.01610.x, 2008. 1918, 1926

Borma, L. S., da Rocha, H. R., Cabral, O. M., von Randow, C., Collicchio, E., Kurzatkowski, D., Brugger, P. J., Freitas, H., Tannus, R., Oliveira, L., Rennó, C. D., and Artaxo, P.: Atmosphere and hydrological controls of the evapotranspiration over a floodplain forest in the Bananal Island region, Amazonia, J. Geophys. Res., 114, G01003, doi:10.1029/2007JG000641, 2009. 1930

Butler, M. P., Davis, K. J., Denning, A. S., and Kawa, S. R.: Using continental observations in global atmospheric inversions of CO_2: North American carbon sources and sinks, Tellus B, 62, 550–572, doi:10.1111/j.1600-0889.2010.00501.x, 2010. 1926

Carswell, F. E., Costa, A. L., Palheta, M., Malhi, Y., Meir, P., Costa, J. d. P. R., Ruivo, M. d. L., Leal, L. d. S. M., Costa, J. M. N., Clement, R. J., and Grace, J.: Seasonality in CO_2 and H_2O flux at an eastern Amazonian rain forest, J. Geophys. Res., 107, LBA 43-1–LBA 43-16, doi:10.1029/2000JD000284, 2002. 1930

Chevallier, F., Viovy, N., Reichstein, M., and Ciais, P.: On the assignment of prior errors in Bayesian inversions of CO_2 surface fluxes, Geophys. Res. Lett., 33, L13802, doi:10.1029/2006GL026496, 2006. 1924

Chevallier, F., Ciais, P., Conway, T. J., Aalto, T., Anderson, B. E., Bousquet, P., Brunke, E. G., Ciattaglia, L., Esaki, Y., Fröhlich, M., Gomez, A., Gomez-Pelaez, A. J., Haszpra, L., Krummel, P. B., Langenfelds, R. L., Leuenberger, M., Machida, T., Maignan, F., Matsueda, H., Morguí, J. A., Mukai, H., Nakazawa, T., Peylin, P., Ramonet, M., Rivier, L., Sawa, Y., Schmidt, M., Steele, L. P., Vay, S. A., Vermeulen, A. T., Wofsy, S., and Worthy, D.: CO_2 surface fluxes at grid point scale estimated from a global 21 year reanalysis of atmospheric measurements, J. Geophys. Res., 115, D21307, doi:10.1029/2010JD013887, 2010. 1921
Ciais, P., Rayner, P., Chevallier, F., Bousquet, P., Logan, M., Peylin, P., and Ramonet, M.: Atmospheric inversions for estimating CO_2 fluxes: methods and perspectives, Climatic Change, 103, 69–92, 2010. 1919
Enting, I. G., Trudinger, C. M., and Francey, R. J.: A synthesis inversion of the concentration and δ^{13}C of atmospheric CO_2, Tellus B, 47, 35–52, 1995. 1919
Gatti, L. V., Miller, J. B., D'Amelio, M. T. S., Martinewski, A., Basso, L. S., Gloor, M. E., Wofsy, S., and Tans, P.: Vertical profiles of CO_2 above eastern Amazonia suggest a net carbon flux to the atmosphere and balanced biosphere between 2000 and 2009, Tellus B, 62, 581–594, doi:10.1111/j.1600-0889.2010.00484.x, 2010. 1920, 1926
Gatti, L. V., Gloor, M., Miller, J. B., Doughty, C. E., Malhi, Y., Domingues, L. G., Basso, L. S., Martinewski, A., Correia, C. S. C., Borges, V. F., Freitas, S., Braz, R., Anderson, L. O., Rocha, H., Grace, J., Phillips, O. L., and Lloyd, J.: Drought sensitivity of Amazonian carbon balance revealed by atmospheric measurements, Nature, 506, 76–80, doi:10.1038/nature12957, 2014. 1920, 1935
Gloor, M., Gatti, L., Brienen, R., Feldpausch, T. R., Phillips, O. L., Miller, J., Ometto, J. P., Rocha, H., Baker, T., de Jong, B., Houghton, R. A., Malhi, Y., Aragão, L. E. O. C., Guyot, J.-L., Zhao, K., Jackson, R., Peylin, P., Sitch, S., Poulter, B., Lomas, M., Zaehle, S., Huntingford, C., Levy, P., and Lloyd, J.: The carbon balance of South America: a review of the status, decadal trends and main determinants, Biogeosciences, 9, 5407–5430, doi:10.5194/bg-9-5407-2012, 2012. 1918, 1920, 1921
Goulden, M. L., Miller, S. D., da Rocha, H. R., Menton, M. C., de Freitas, H. C., e Silva Figueira, A. M., and de Sousa, C. A. D.: Diel and seasonal patterns of tropical forest CO_2 exchange, Ecol. Appl., 14, 42–54, doi:10.1890/02-6008, 2004. 1930
Grace, J., Malhi, Y., Lloyd, J., McIntyre, J., Miranda, A. C., Meir, P., and Miranda, H. S.: The use of eddy covariance to infer the net carbon dioxide uptake of Brazilian rain forest, Glob. Change Biol., 2, 209–217, doi:10.1111/j.1365-2486.1996.tb00073.x, 1996. 1918

ACPD
15, 1915–1952, 2015

On the ability of a global atmospheric inversion to constrain variations of CO_2 fluxes over Amazonia

L. Molina et al.

Hourdin, F., Musat, I., Bony, S., Braconnot, P., Codron, F., Dufresne, J.-L., Fairhead, L., Filiberti, M.-A., Friedlingstein, P., Grandpeix, J.-Y., Krinner, G., LeVan, P., Li, Z.-X., and Lott, F.: The LMDZ4 general circulation model: climate performance and sensitivity to parametrized physics with emphasis on tropical convection, Clim. Dynam., 27, 787–813, doi:10.1007/s00382-006-0158-0, 2006. 1923

Huete, A. R., Didan, K., Shimabukuro, Y. E., Ratana, P., Saleska, S. R., Hutyra, L. R., Yang, W., Nemani, R. R., and Myneni, R.: Amazon rainforests green-up with sunlight in dry season, Geophys. Res. Lett., 33, L06405, doi:10.1029/2005GL025583, 2006. 1918

INPE: Projeto de Monitoramento do Desmatamento na Amazônia Legal por Satélite (PRODES), available at: http://www.obt.inpe.br/prodes/index.php (last access: 4 May 2014), 2011. 1917

Jung, M., Reichstein, M., Margolis, H. A., Cescatti, A., Richardson, A. D., Arain, M. A., Arneth, A., Bernhofer, C., Bonal, D., Chen, J., Gianelle, D., Gobron, N., Kiely, G., Kutsch, W., Lasslop, G., Law, B. E., Lindroth, A., Merbold, L., Montagnani, L., Moors, E. J., Papale, D., Sottocornola, M., Vaccari, F., and Williams, C.: Global patterns of land–atmosphere fluxes of carbon dioxide, latent heat, and sensible heat derived from eddy covariance, satellite, and meteorological observations, J. Geophys. Res., 116, G00J07, doi:10.1029/2010JG001566, 2011. 1921

Krinner, G., Viovy, N., de Noblet-Ducoudré, N., Ogée, J., Polcher, J., Friedlingstein, P., Ciais, P., Sitch, S., and Prentice, I. C.: A dynamic global vegetation model for studies of the coupled atmosphere–biosphere system, Global Biogeochem. Cy., 19, GB1015, doi:10.1029/2003GB002199, 2005. 1922

Lewis, S. L., Brando, P. M., Phillips, O. L., van der Heijden, G. M. F., and Nepstad, D.: The 2010 Amazon drought, Science, 331, p. 554, doi:10.1126/science.1200807, 2011. 1931, 1935

Lloyd, J., Kolle, O., Fritsch, H., de Freitas, S. R., Silva Dias, M. A. F., Artaxo, P., Nobre, A. D., de Araújo, A. C., Kruijt, B., Sogacheva, L., Fisch, G., Thielmann, A., Kuhn, U., and Andreae, M. O.: An airborne regional carbon balance for Central Amazonia, Biogeosciences, 4, 759–768, doi:10.5194/bg-4-759-2007, 2007. 1920

Maignan, F., Bréon, F.-M., Chevallier, F., Viovy, N., Ciais, P., Garrec, C., Trules, J., and Mancip, M.: Evaluation of a Global Vegetation Model using time series of satellite vegetation indices, Geosci. Model Dev., 4, 1103–1114, doi:10.5194/gmd-4-1103-2011, 2011. 1923

Malhi, Y., Roberts, J. T., Betts, R. A., Killeen, T. J., Li, W., and Nobre, C. A.: Climate change, deforestation, and the fate of the Amazon, Science, 319, 169–172, 2008. 1917

ACPD
15, 1915–1952, 2015

On the ability of a global atmospheric inversion to constrain variations of CO_2 fluxes over Amazonia

L. Molina et al.

Malhi, Y., Aragão, L. E. O. C., Galbraith, D., Huntingford, C., Fisher, R., Zelazowski, P., Sitch, S., McSweeney, C., and Meir, P.: Exploring the likelihood and mechanism of a climate-change-induced dieback of the Amazon rainforest, P. Natl. Acad. Sci. USA, 106, 20610–20615, doi:10.1073/pnas.0804619106, 2009. 1931

Marengo, J. A., Ronchail, J., Baez, J., and Alves, L.: State of the climate in 2009, in: The Climate of Tropical South America East of the Andes, vol. 91, American Meteorological Society, Boston, MA, USA, S148–S150, 2010. 1921

Miller, S. D., Goulden, M. L., Menton, M. C., da Rocha, H. R., de Freitas, H. C., Figueira, A. M. E. S., and Dias de Sousa, C. A.: Biometric and micrometeorological measurements of tropical forest carbon balance, Ecol. Appl., 14, 114–126, doi:10.1890/02-6005, 2004. 1930

Moreira, D. S., Freitas, S. R., Bonatti, J. P., Mercado, L. M., Rosário, N. M. É., Longo, K. M., Miller, J. B., Gloor, M., and Gatti, L. V.: Coupling between the JULES land-surface scheme and the CCATT-BRAMS atmospheric chemistry model (JULES-CCATT-BRAMS1.0): applications to numerical weather forecasting and the CO_2 budget in South America, Geosci. Model Dev., 6, 1243–1259, doi:10.5194/gmd-6-1243-2013, 2013. 1935

Morton, D. C., Nagol, J., Carabajal, C. C., Rosette, J., Palace, M., Cook, B. D., Vermote, E. F., Harding, D. J., and North, P. R. J.: Amazon forests maintain consistent canopy structure and greenness during the dry season, Nature, 506, 7487, doi:10.1038/nature13006, 2014. 1919

Negrón-Juárez, R. I., Chambers, J. Q., Guimaraes, G., Zeng, H., Raupp, C. F. M., Marra, D. M., Ribeiro, G. H. P. M., Saatchi, S. S., Nelson, B. W., and Higuchi, N.: Widespread Amazon forest tree mortality from a single cross-basin squall line event, Geophys. Res. Lett., 37, L16701, doi:10.1029/2010GL043733, 2010. 1935

Olivier, J. and Berdowski, J.: Global emissions sources and sinks, in: The Climate System, A. A. Balkema Publishers/Swets & Zeitlinger Publishers, Lisse, 33–78, 2001. 1923

Ometto, J. P. H. B., Nobre, A. D., Rocha, H. R., Artaxo, P., and Martinelli, L. A.: Amazonia and the modern carbon cycle: lessons learned, Oecologia, 143, 483–500, 2005. 1919

Parazoo, N. C., Denning, A. S., Kawa, S. R., Corbin, K. D., Lokupitiya, R. S., and Baker, I. T.: Mechanisms for synoptic variations of atmospheric CO_2 in North America, South America and Europe, Atmos. Chem. Phys., 8, 7239–7254, doi:10.5194/acp-8-7239-2008, 2008. 1935

Parazoo, N. C., Bowman, K., Frankenberg, C., Lee, J.-E., Fisher, J. B., Worden, J., Jones, D. B. A., Berry, J., Collatz, G. J., Baker, I. T., Jung, M., Liu, J., Osterman, G., O'Dell, C., Sparks, A., Butz, A., Guerlet, S., Yoshida, Y., Chen, H., and Gerbig, C.: Interpreting seasonal changes in the carbon balance of southern Amazonia using measurements of XCO_2 and chlorophyll fluorescence from GOSAT, Geophys. Res. Lett., 40, 2829–2833, doi:10.1002/grl.50452, 2013. 1918

Peylin, P., Baker, D., Sarmiento, J., Ciais, P., and Bousquet, P.: Influence of transport uncertainty on annual mean and seasonal inversions of atmospheric CO_2 data, J. Geophys. Res., 107, 4385, doi:10.1029/2001JD000857, 2002. 1932, 1934

Peylin, P., Law, R. M., Gurney, K. R., Chevallier, F., Jacobson, A. R., Maki, T., Niwa, Y., Patra, P. K., Peters, W., Rayner, P. J., Rödenbeck, C., van der Laan-Luijkx, I. T., and Zhang, X.: Global atmospheric carbon budget: results from an ensemble of atmospheric CO_2 inversions, Biogeosciences, 10, 6699–6720, doi:10.5194/bg-10-6699-2013, 2013. 1920

Phillips, O. L., Aragão, L. E. O. C., Lewis, S. L., Fisher, J. B., Lloyd, J., López-González, G., Malhi, Y., Monteagudo, A., Peacock, J., Quesada, C. A., van der Heijden, G., Almeida, S., Amaral, I., Arroyo, L., Aymard, G., Baker, T. R., Bánki, O., Blanc, L., Bonal, D., Brando, P., Chave, J., de Oliveira, A. C. A., Cardozo, N. D., Czimczik, C. I., Feldpausch, T. R., Freitas, M. A., Gloor, E., Higuchi, N., Jiménez, E., Lloyd, G., Meir, P., Mendoza, C., Morel, A., Neill, D. A., Nepstad, D., Patiño, S., Peñuela, M. C., Prieto, A., Ramírez, F., Schwarz, M., Silva, J., Silveira, M., Thomas, A. S., Steege, H. T., Stropp, J., Vásquez, R., Zelazowski, P., Dávila, E. A., Andelman, S., Andrade, A., Chao, K.-J., Erwin, T., Di Fiore, A. C. E. H., Keeling, H., Killeen, T. J., Laurance, W. F., Cruz, A. P., Pitman, N. C. A., Vargas, P. N., Ramírez-Angulo, H., Rudas, A., Salamão, R., Silva, N., Terborgh, J., and Torres-Lezama, A.: Drought sensitivity of the Amazon rainforest, Science, 323, 1344–1347, 2009. 1919

Poulter, B., Heyder, U., and Cramer, W.: Modeling the sensitivity of the seasonal cycle of GPP to dynamic LAI and soil depths in tropical rainforests, Ecosystems, 12, 517–533, doi:10.1007/s10021-009-9238-4, 2009. 1918

Randerson, J. T., van der Werf, G. R., Giglio, L., Collatz, G. J., and Kasibhatla, P. S.: Global Fire Emissions Database, Version 2.1. Data set from Oak Ridge National Laboratory Distributed Active Archive Center, Oak Ridge, Tennessee, USA, doi:10.3334/ORNLDAAC/849, available at: http://daac.ornl.gov/ (last access: 9 September 2013), 2007. 1923

Saatchi, S., Asefi-Najafabady, S., Malhi, Y., Aragão, L. E. O. C., Anderson, L. O., Myneni, R. B., and Nemani, R.: Persistent effects of a severe drought on Amazonian forest canopy, P. Natl. Acad. Sci. USA, 110, 565–570, 2012. 1919

Saleska, S. R., Miller, S. D., Matross, D. M., Goulden, M. L., Wofsy, S. C., da Rocha, H. R., de Camargo, P. B., Crill, P., Daube, B. C., de Freitas, H. C., Hutyra, L., Keller, M., Kirchhoff, V., Menton, M., Munger, J. W., Pyle, E. H., Rice, A. H., and Silva, H.: Carbon in Amazon forests: unexpected seasonal fluxes and disturbance-induced losses, Science, 302, 1554–1557, 2003. 1918

Saleska, S. R., Didan, K., Huete, A. R., and da Rocha, H. R.: Amazon forests green-up during 2005 drought, Science, 318, 612–612, 2007. 1919

Samanta, A., Ganguly, S., Hashimoto, H., Devadiga, S., Vermote, E., Knyazikhin, Y., Nemani, R. R., and Myneni, R. B.: Amazon forests did not green-up during the 2005 drought, Geophys. Res. Lett., 37, L05401, doi:10.1029/2009GL042154, 2010. 1919

Samanta, A., Ganguly, S., Vermote, E., Nemani, R. R., and Myneni, R. B.: Interpretation of variations in MODIS-measured greenness levels of Amazon forests during 2000 to, Environ. Res. Lett., 7, 024018, doi:10.1088/1748-9326/7/2/024018, 2012. 1919

Takahashi, T., Sutherland, S. C., Wanninkhof, R., Sweeney, C., Feely, R. A., Chipman, D. W., Hales, B., Friederich, G., Chavez, F., Sabine, C., Watson, A., Bakker, D. C., Schuster, U., Metzl, N., Yoshikawa-Inoue, H., Ishii, M., Midorikawa, T., Nojiri, Y., Körtzinger, A., Steinhoff, T., Hoppema, M., Olafsson, J., Arnarson, T. S., Tilbrook, B., Johannessen, T., Olsen, A., Bellerby, R., Wong, C., Delille, B., Bates, N., and de Baar, H. J.: Climatological mean and decadal change in surface ocean pCO_2, and net sea–air CO_2 flux over the global oceans, Deep-Sea Res. Pt. II, 56, 554–577, 2009. 1923

Tarantola, A.: Inverse Problem Theory and Methods for Model Parameter Estimation, Society for Industrial and Applied Mathematics, Philadelphia, 2005. 1922

Verbeeck, H., Peylin, P., Bacour, C., Bonal, D., Steppe, K., and Ciais, P.: Seasonal patterns of CO_2 fluxes in Amazon forests: fusion of eddy covariance data and the ORCHIDEE model, J. Geophys. Res., 116, G02018, doi:10.1029/2010JG001544, 2011. 1918

von Randow, C., Manzi, A. O., Kruijt, B., de Oliveira, P. J., Zanchi, F. B., Silva, R. L., Hodnett, M. G., Gash, J. H. C., Elbers, J. A., Waterloo, M. J., Cardoso, F. L., and Kabat, P.: Comparative measurements and seasonal variations in energy and carbon exchange over forest and pasture in south west Amazonia, Theor. Appl. Climatol., 78, 5–26, doi:10.1007/s00704-004-0041-z, 2004. 1930

Wang, W., Ciais, P., Nemani, R. R., Canadell, J. G., Piao, S., Sitch, S., White, M. A., Hashimoto, H., Milesi, C., and Myneni, R. B.: Variations in atmospheric CO_2 growth rates coupled with tropical temperature, P. Natl. Acad. Sci. USA, 110, 13061–13066, doi:10.1073/pnas.1219683110, 2013. 1918

ACPD
15, 1915–1952, 2015

Xu, L., Samanta, A., Costa, M. H., Ganguly, S., Nemani, R. R., and Myneni, R. B.: Widespread decline in greenness of Amazonian vegetation due to the 2010 drought, Geophys. Res. Lett., 38, L07402, doi:10.1029/2011GL046824, 2011. 1919

ACPD
15, 1915–1952, 2015

On the ability of a global atmospheric inversion to constrain variations of CO_2 fluxes over Amazonia

L. Molina et al.

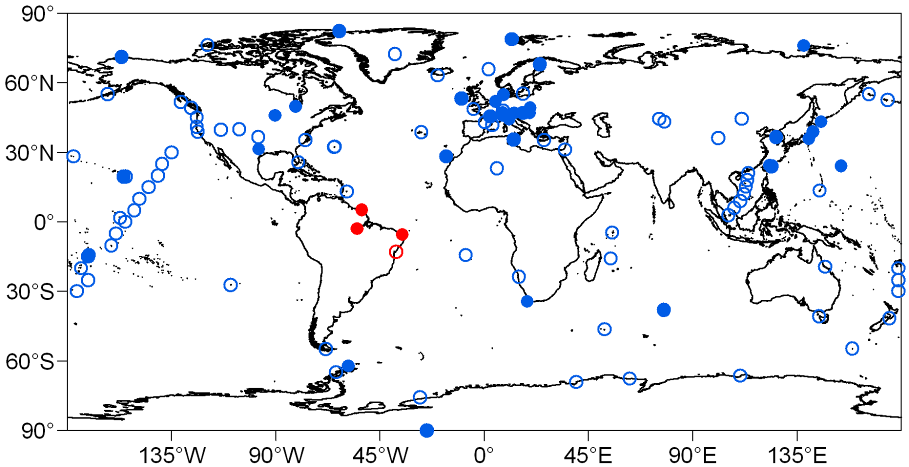

Figure 1. Location of the surface stations used in this study. Blue: surface stations used in CH2010, red: surface stations in South America added to the previous setup of CH2010. Filled circles: stations with continuous measurements, open circles: sites with discrete air sampling.

ACPD
15, 1915–1952, 2015

On the ability of a global atmospheric inversion to constrain variations of CO_2 fluxes over Amazonia

L. Molina et al.

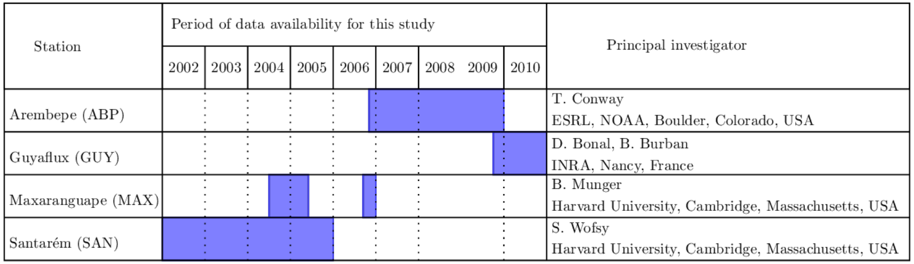

Figure 2. List of surface stations over South America added to the previous setup of Chevallier et al. (2010).

ACPD
15, 1915–1952, 2015

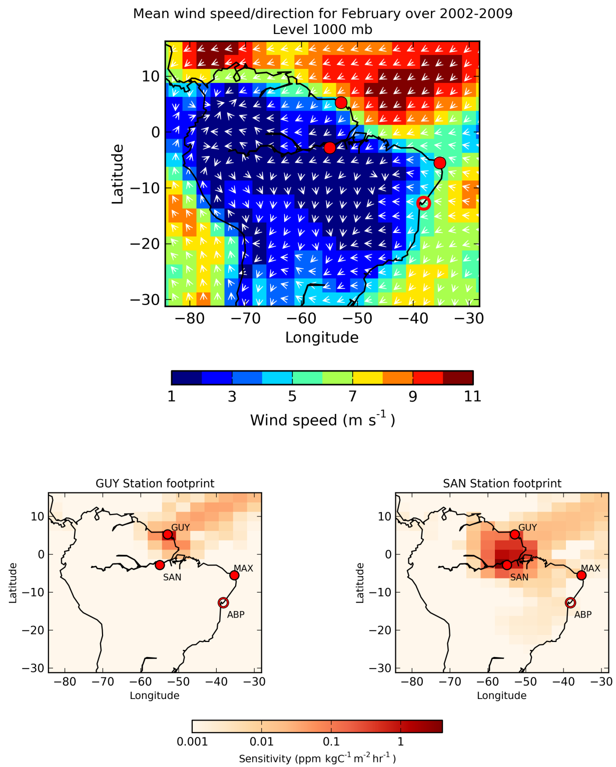

Figure 3. Top: Location of assimilated surface stations in South America and mean wind speed/direction for February, averaged over 2002–2010 (Source: NCEP/NCAR Reanalysis). Sensitivity of surface atmospheric CO_2 mole fractions measured on 20 February 2009 at 10:00 UTC, at Guyaflux (left) and Santarém (right), to a constant increment of surface fluxes during the two days prior to the measurement. Sensitivity values are expressed in log-scale. Open circles: sites with discrete air samplings. Filled circles: measurements taken with continuous analyzers.

ACPD
15, 1915–1952, 2015

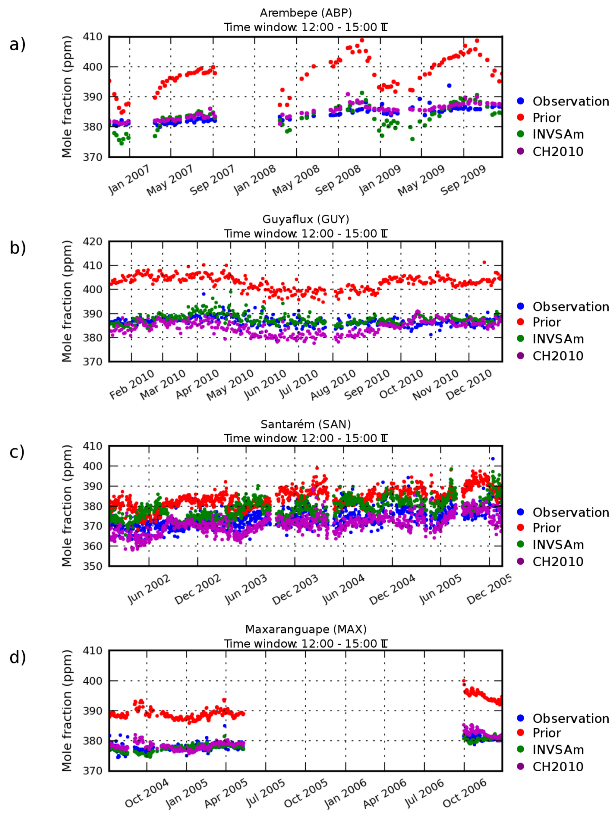

Figure 4. Comparison of assimilated CO_2 observations (blue) and corresponding simulated mole fractions using prior fluxes (red), INVSAm (green) and CH2010 (purple). Measurements were collected at Arembepe **(a)**, Guyaflux **(b)**, Santarém **(c)** and Maxaranguape **(d)**. Data shown here correspond to daily average mole fractions between 12:00 and 15:00 local time (LT), when wind speed $> 2\,\mathrm{m\,s^{-1}}$. Note that the time scale differs between plots.

ACPD
15, 1915–1952, 2015

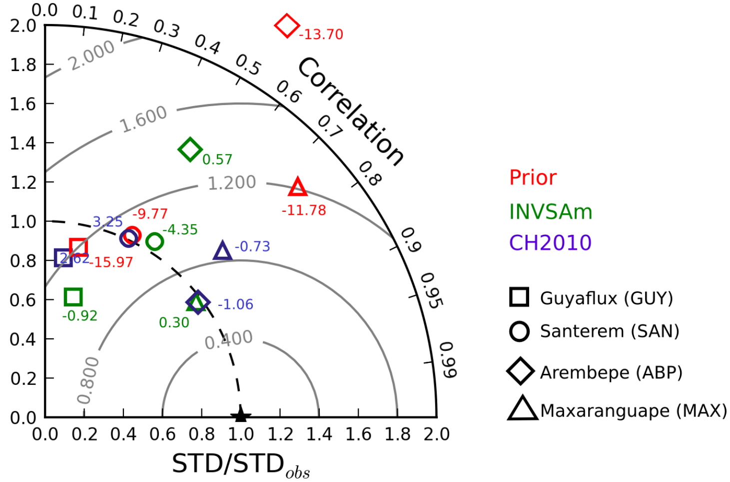

Figure 5. Taylor diagram of the statistics of misfits between observations and simulated CO_2 mole fractions between 12:00 and 15:00 LT at Guyaflux (square), Santarém (circle), Arembepe (diamond) and Maxaranguape (triangle), when wind speed $> 2\,m\,s^{-1}$, using prior fluxes (red), INVSAm (green) and CH2010 (purple). Radial distance from the origin: ratio of SD of simulated mole fractions and SD of the observations. Angle measured from the y axis: coefficient of correlation. Numbers next to the symbols: bias (in ppm). Gray circles: SD of the misfits (in ppm).

ACPD
15, 1915–1952, 2015

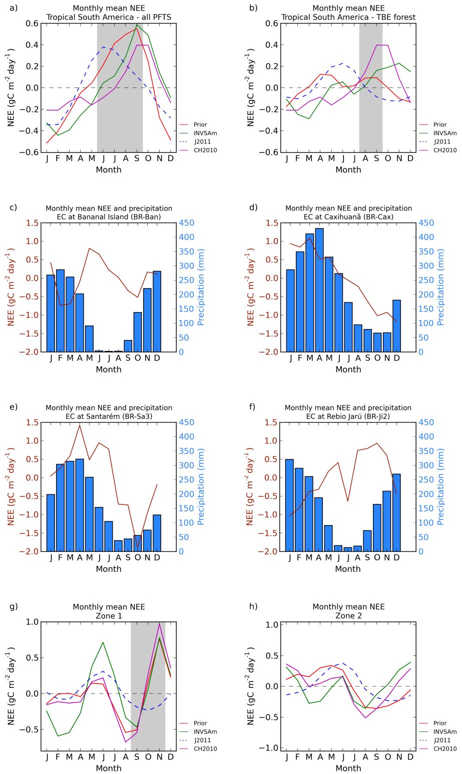

Figure 6. Monthly mean NEE integrated over **(a)** the whole study region and **(b)** over pixels dominated by TBE forests in ORCHIDEE for 2002–2010. The shaded areas denote dry seasons, defined as months with precipitation < 100 mm, based on monthly totals from TRMM data over 2002–2010. Estimates from prior fluxes (red), INVSAm (green), CH2010 (purple) and J2011 (dashed blue). **(c–f)** Monthly mean NEE measurements from EC stations at **(c)** Bananal Island (2004–2005), **(d)** Caxihuanã (2000–2002), **(e)** Rebio Jarú (2000–2002), and Santarém (2001–2002). **(g–h)** Monthly mean NEE integrated over the zones 1 **(g)** and 2 **(h)** that are defined in Fig. 7.

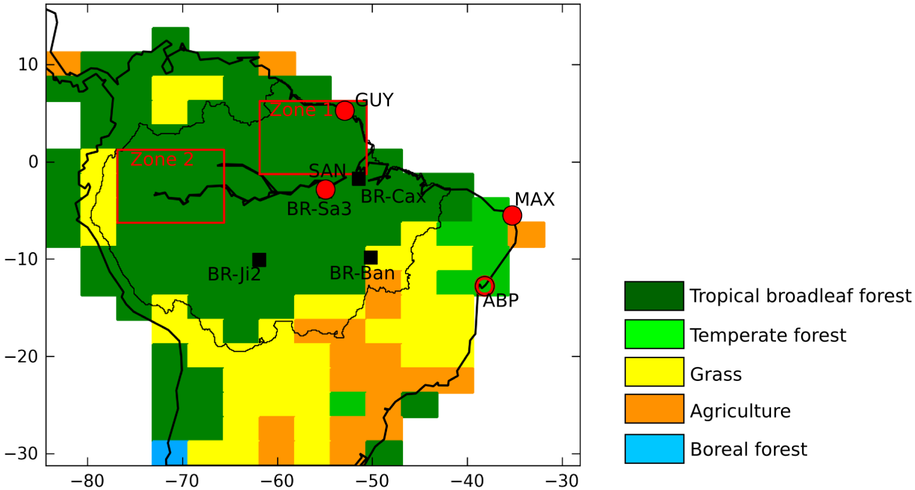

Figure 7. Dominating PFTs for each transport model grid cell (i.e. 3.75° × 2.50°) according to the ORCHIDEE vegetation map over the study region. Open circles show location of sites with discrete air sampling; filled circles show location of sites with continuous measurements; and squares show locations of the EC measurement stations used in this study. Zones 1 and 2 indicate areas for which the NEE is presented in Figs. 6g and h, 10.

ACPD
15, 1915–1952, 2015

On the ability of a global atmospheric inversion to constrain variations of CO_2 fluxes over Amazonia

L. Molina et al.

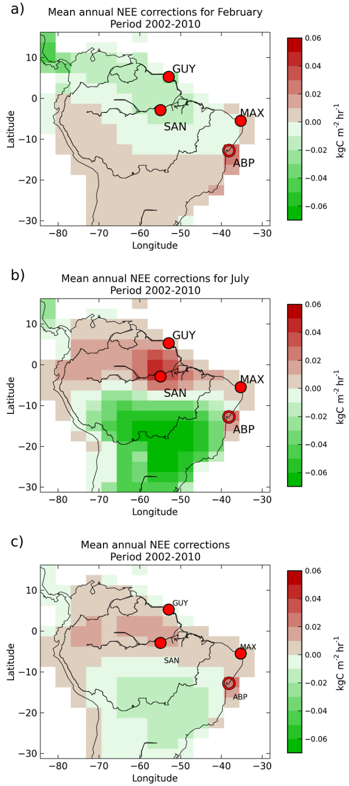

Figure 8. Spatial distribution of 2002–2010 mean flux corrections at the transport model resolution (3.75° × 2.50°) to ORCHIDEE from INVSAm over the study region: mean for **(a)** February, **(b)** July, and **(c)** mean over the full period 2002–2010. Filled circles indicate locations of sites with continuous measurements; and open circles indicate locations of sites with discrete air sampling.

ACPD
15, 1915–1952, 2015

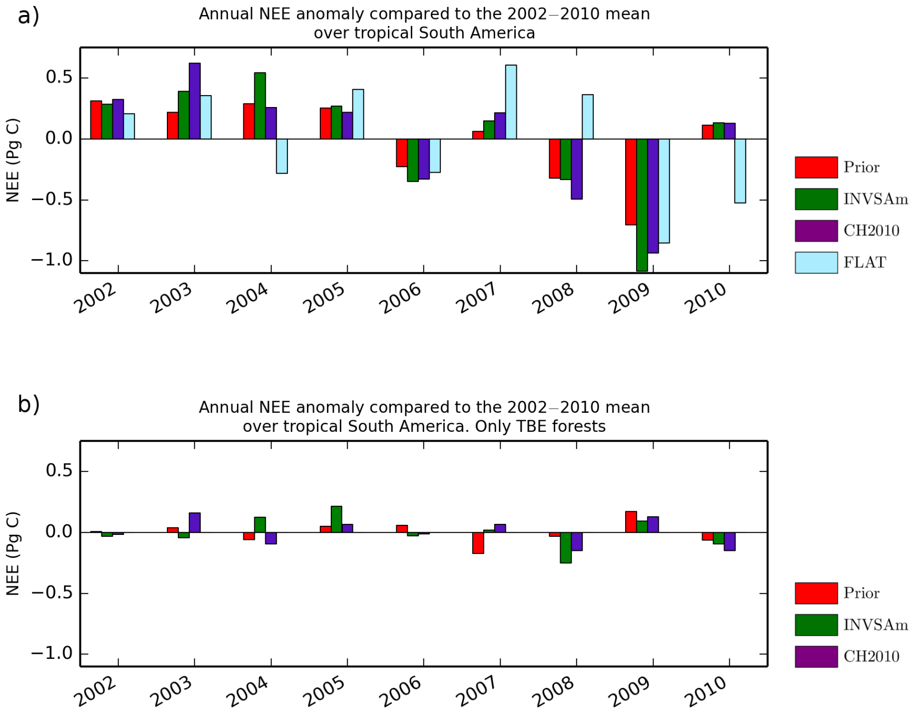

Figure 9. (a) Annual NEE anomaly compared to the mean of 2002–2010; estimates for the whole study region. **(b)** Annual NEE anomaly compared to the mean of 2002–2010; estimates for the area dominated by TBE forests.

ACPD
15, 1915–1952, 2015

On the ability of a global atmospheric inversion to constrain variations of CO_2 fluxes over Amazonia

L. Molina et al.

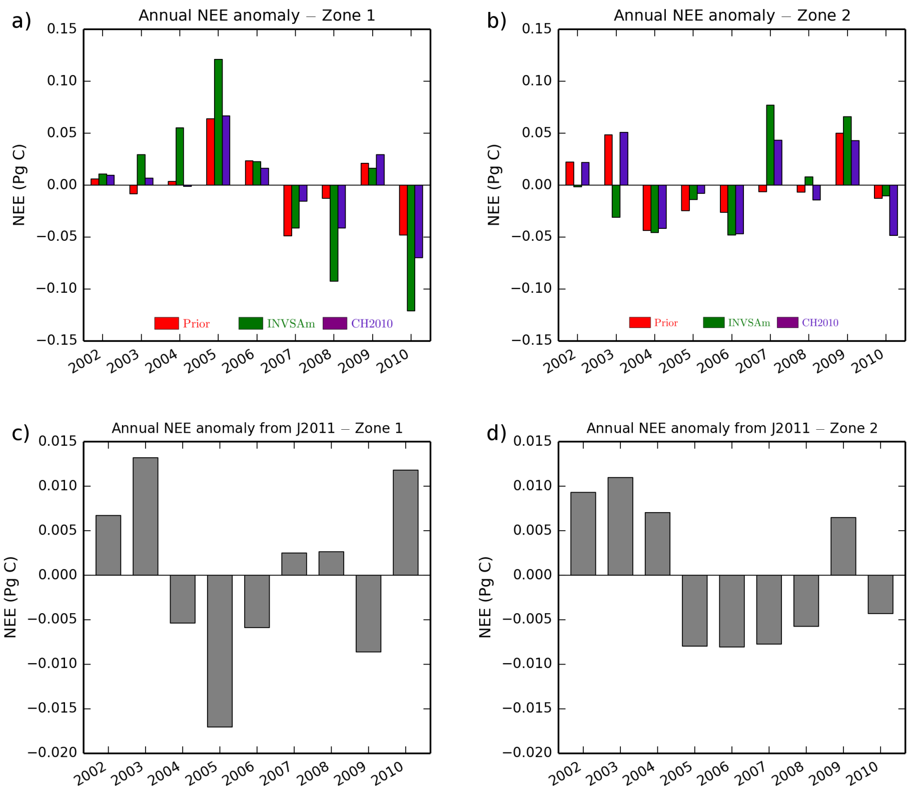

Figure 10. Annual NEE anomaly compared to the 2002–2010 mean for Zone 1 **(a, c)** and Zone 2 **(b, d)** as defined in Fig. 7. Estimates from prior fluxes (red), INVSAm (green), CH2010 (purple), and J2011 (gray).

ACPD
15, 1915–1952, 2015

On the ability of a global atmospheric inversion to constrain variations of CO_2 fluxes over Amazonia

L. Molina et al.